JMEPEG (2013) 22:184–189
DOI: 10.1007/s11665-012-0228-x

1059-9495/$19.00

Transport Properties of Carbon-Nanotube/Cement Composites

Baoguo Han, Zhengxian Yang, Xianming Shi, and Xun Yu

(Submitted October 3, 2011; in revised form February 29, 2012; published online April 11, 2012)

This paper preliminarily investigates the general transport properties (i.e., water sorptivity, water permeability, and gas permeability) of carbon-nanotube/cement composites. Carboxyl multi-walled carbon nanotubes (MWNTs) are dispersed into cement mortar to fabricate the carbon nanotubes (CNTs) reinforced cement-based composites by applying ultrasonic energy in combination with the use of surfactants (sodium dodecylbenzene sulfonate and sodium dodecyl sulfate). Experimental results indicate that even at a very small dosage the addition of MWNTs can help decrease water sorptivity coefficient, water permeability coefficient, and gas permeability coefficient of cement mortar, which suggests that CNTs can effectively improve the durability properties of cement-based composites.

Keywords carbon nanotubes, cement-based composites, durability, permeability, water sorptivity

1. Introduction

A significant portion of the current civil infrastructure is partially or completely constructed out of cement-based materials such as concrete. Cement-based materials are typically characterized as quasi-brittle materials with low tensile strength and low strain capacity. Fibers can be incorporated into cement-based materials to overcome these weaknesses. Typical reinforcement of cement-based materials is provided using reinforcing bars and macrofibers, which reinforce cement-based materials on the centimeter or millimeter scale. Recently, the use of microfiber reinforcement has led to significant improvement of the mechanical properties of cement-based materials. However, while microfibers delay the development of formed microcracks and enhance the energy absorption and ductility of the cementitious composite through crack bridging, they do not stop their initiation (Ref 1). The development of new nanosized fibers has opened a new field for nanosized reinforcement within cement-based materials. Nanofibers can not only improve the fracture properties of cementitious matrix by controlling the cracks at the nanoscale level but also improve the early age strain capacity of the cementitious matrix (thus preventing the crack initiation) whereas microfibers reinforce concrete by delaying the development of formed microcracks (Ref 2-4).

Carbon nanotubes (CNTs) are considered one of the most beneficial nanomaterials for reinforcement on the nanometer scale with amazing mechanical properties (e.g., ultra-high strength and stiffness, and elastic stress-strain behavior) (Ref 4-7). The Young's modulus of the best CNTs can be as high as 1000 GPa which is approximately 5 times higher than steel. The tensile strength of CNTs can be up to 63 GPa, around 50 times higher than steel. In addition to their high strength and elastic constant, CNTs have extremely high aspect ratios, with values typically higher than 1000:1 and reaching as high as 2,500,000:1. As a result of these properties coupled with the lightness, large surface area (typically 200-300 m^2/g), and excellent chemical and thermal stability, CNTs reinforcements are expected to produce significantly stronger and tougher cement-based materials than traditional reinforcing materials (e.g., glass fibers or carbon fibers) (Ref 8). The CNTs' reinforcement capability to the CNTs-reinforced cement-based composites depends on many factors, among them the quality of CNTs' dispersion, the final aspect ratio (whether the nanotubes were shortened as a result of disaggregation treatment), CNTs' concentration level, CNTs' intrinsic structure and properties, composition and structure of matrix, and the interfacial bonding condition between CNTs and matrix. Therefore, very different results have been reported on the mechanical behavior of CNTs-reinforced cement-based composites. The best observed performances include a 50% increase in compressive strength in a multi-walled carbon nanotubes (MWNTs)-reinforced cement-based composite (Ref 9), over 600% improvement in Vickers's hardness at early ages of hydration for a SWNTs-reinforced cement-based composite (Ref 8), a 227% increase in Young's modulus for a MWNTs-reinforced cement-based composite (Ref 10) and a 40% increase in flexural strength for a MWNTs-reinforced

Baoguo Han and Zhengxian Yang have equal contribution to the paper.

Baoguo Han, Department of Mechanical and Energy Engineering, University of North Texas, Denton, TX 76203; and School of Civil Engineering, Harbin Institute of Technology, Harbin 150090, China; **Zhengxian Yang**, Corrosion and Sustainable Infrastructure Laboratory, Western Transportation Institute, College of Engineering, Montana State University, P.O. Box 174250, Bozeman, MT 59717-4250; and Department of Materials and Environment, Faculty of Civil Engineering and Geosciences, Delft University of Technology, 2628CN Delft, The Netherlands; **Xianming Shi**, Corrosion and Sustainable Infrastructure Laboratory, Western Transportation Institute, College of Engineering, Montana State University, P.O. Box 174250, Bozeman, MT 59717-4250; and **Xun Yu**, Department of Mechanical and Energy Engineering, University of North Texas, Denton, TX 76203. Contact e-mails: xianming_s@ coe.motnana.edu and xun.yu@unt.edu.

cement-based composite (Ref 2). The investigations of microstructure have indicated that if the nanotubes are well dispersed there may be potential for improving the mechanical properties of cement-based materials in a more consistent way. The use of CNTs can strongly reinforce the cement-based materials at the nanoscale by increasing the amount of high stiffness C-S-H and decreasing the porosity which leads to the reduction of the autogenous shrinkage. Surprisingly, the addition of CNTs also controls the formation of matrix cracks at the nanoscale level (Ref 2). Evidence for crack bridging in MWNTs-reinforced cement-based composites has been observed. Other forms of classical reinforcing behaviors such as fiber-pullout and crack deflection have also been observed (Ref 8).

In addition to the mechanical studies, work has been undertaken on the electrical properties of CNTs-reinforced cement-based composites. The researchers found significant improvements in electrical conductivity as compared to control samples, the measured values are much higher than the level of conductivity that should be expected based on the level of loading of CNTs in the composites (Ref 4). Additionally, as the CNTs-reinforced cement-based composites are deformed or stressed, the contact state between the nanotubes and the matrix is changed, which affects the electrical resistance of the composites. Strain, stress, crack, and damage of the composites can therefore be detected through measurement of the electrical resistance (Ref 11-13). Besides mechanical, electrical, and sensing properties, CNTs-reinforced cement-based composites have other functional properties, such as thermal conductive property and damping property (Ref 14, 15).

Transport properties define the rate of ingress of deleterious species (e.g., water, chlorides, and sulfate) from the service environment into the cement-based structures and components throughout their service life. They are intrinsic durability properties to be considered at the materials research and structural design stages (Ref 16). Chen et al. (Ref 17) comprehensively reviewed the beneficial effects of CNTs on the hydration process of CNTs filled cement composites and the hydration products, pore structures, autogenous shrinkage, and transport of water and iron in the composites. It is expected that CNTs-reinforced cement-based composites would exhibit improved transport properties relative to the conventional cement-based composites. In this paper, water sorptivity, water permeability, and gas permeability are investigated, as they are important parameters characterizing the general transport properties of cementitious materials. Sodium dodecylbenzene sulfonate (NaDDBS) and sodium dodecyl sulfate (SDS) are used as surfactants to improve the dispersion of MWNTs in cement mortar and to facilitate the fabrication of CNTs-reinforced cement mortar composites.

2. Materials and Experimental Method

2.1 Materials

The cement used is Portland cement (ASTM Type I) provided by Holcim Inc., Waltham, MA, USA. The sand used is commercial grade fine sand provided by Quikrete International Inc., Atlanta, GA, USA. Musso et al. (Ref 18) stated that the carboxyl MWNTs led to a worsening in mechanical properties of cement-based composites, but some other studies proved that the carboxyl CNTs are much easier to disperse in water and cement matrix than the plain CNTs. Moreover, the carboxyl CNTs have better bond with cement matrix than the plain CNTs (Ref 13, 17). Therefore, the carboxyl MWNTs are used in this study. They are provided by Timesnano, Chengdu Organic Chemicals Co. Ltd. of Chinese Academy of Sciences, Chengdu, China. Their properties are given in Table 1. The surfactants used for dispersing the MWNTs are SDS and NaDDBS, both provided by Sigma-Aldrich Co., Saint Louis, MO, USA. Tributyl phosphate (Sigma-Aldrich Co., MO, USA, USA) is used as defoamer to suppress the production of air bubble in CNTs-reinforced cement mortar composites caused by the use of NaDDBS and SDS.

2.2 Sample Preparation

Previous studies have proved that the dispersing capability of surfactant to CNTs increases with the ratio of surfactant to CNTs (Ref 19-21), but an excessive concentration of surfactants has negative effect on the hydration of cement. The critical micelle concentrations in water of NaDDBS and SDS therefore were taken as the input surfactant concentration, respectively. Table 2 describes the mix proportions of the three types of CNTs-reinforced cement mortar composites in this study. The surfactant was first mixed with water using a magnetic stirrer (PC-210, Corning Inc., Corning, NY, USA) for 3 min. Next, MWNTs were added into this aqueous solution and sonicated with an ultrasonicator (2510, Branson Ultrasonic Co., Danbury, CT, USA) for 2 h to make a uniformly dispersed

Table 1 Properties of carboxyl MWNTs

Outside diameter	Inside diameter	-COOH content	Length	Special surface area	Electrical conductivity	Density
<8 nm	2-5 nm	3.86 wt.%	10-30 μm	>500 m^2/g	$>10^2$ s/cm	~2.1 g/cm^3

Table 2 Mix proportions of three types of CNTs-reinforced cement-based composites

Samples	CNTs weight percentage in cement, %	Water-to-cement ratio	Surfactants		Ratio of sand to cement	Defoamer content, vol.%
			Types	Concentration, mol/L		
#0	0	0.46	…		1.5	…
#1	0.2	0.46	NaDDBS	8.1×10^{-3}	1.5	0.25
#2	0.2	0.46	SDS	1.4×10^{-2}	1.5	0.25

suspension. Then, a mortar mixer was used to mix this suspension (or water for the cement-based composites without CNTs), cement and sand for about 3 min. Finally, a defoamer was added into the mixture and mixed for another 3 min.

After pouring the mixes into oiled molds ($5.08 \times 5.08 \times 5.08$ cm), an electric vibrator was used to ensure good compaction. The specimens were then surface-smoothed, and covered with plastic films. All specimens were demolded after 24 h and then cured under the standard condition at a temperature of 20 °C and a relative humidity of 100% for additional 27 days. In order to check the dispersion of CNTs, we tested the discreteness of electrical resistance of the specimens made of the same types of CNTs-reinforced cement-based composites. The maximum standard deviation of electrical resistance of the three types of specimens is 8.6%. This indicates that the above fabrication progress is effective for dispersing CNTs in cement-matrix. For each type of transport property test, two or more specimens from the same mixing design were tested to ensure the statistical reliability of the test results.

2.3 Measurement

2.3.1 Water Sorptivity Test. The water sorptivity test was carried out to determine the rate of absorption of water by hydraulic cement-based composites and study the effect of CNTs on the development of the capillary pores and the capillary water suction of cement-based composites (Ref 22, 23). The specimens used were 10 mm thick cut from the middle of a $50 \times 50 \times 50$ mm cubic sample. To ensure the initial moisture content and its uniformity throughout the specimen under test. The specimens were oven-dried at 105 °C for 24 h and then placed in an environmental chamber at a temperature of 50 ± 2 °C and RH of $80 \pm 3\%$ for 3 days. Afterward, the specimens were placed into a sealable container at 23 ± 2 °C for 15 days before tests begin. Each specimen was placed in a separate container to allow free flow of air around the specimens.

The test was performed by allowing one surface of the specimen to be in contact with water of 10 mm depth using a circular plexiglas support as shown in Fig. 1. Using the supporting frame and keeping the outside water level at 1-3 mm above the top of plexiglas support allows continuous contact between the specimen surface and the water without changing the water depth throughout the test. The sides of the test samples were carefully sealed to create unidirectional flow through the samples. The weight of the specimen was recorded at fixed time intervals. The sorptivity coefficient k_s ($g/cm^2 \cdot s^{1/2}$) was then determined using the following equation:

$$Q/A = k_s\sqrt{t} \quad \text{(Eq 1)}$$

where Q is the amount of water absorbed (g), A is the cross-sectional area of the specimen that was in contact with water (cm^2), and t is the time (s).

2.3.2 Water Permeability Test. The water permeability test was conducted using a falling head test setup as shown in Fig. 2. The specimens used were 10 mm thick cut from a $50 \times 50 \times 50$ mm cubic sample. Prior to the start of the test, a vacuum of approximately 1 mmHg (133 MPa) was applied to the samples in a clean dry vacuum desiccator for 3 h. Then deionized water was added to cover the samples, and the vacuum was maintained for one more hour, after which the vacuum was turned off and the samples were left in the water for another 18 h. On the completion of saturation, the specimen was removed from the desiccator and lightly patted with paper towel. The sides of the samples were sealed using sealant and then the whole testing setup was assembled to start the test. The water drop was measured every 24 h for the first week, then once every 2 days for the remainder of the experiment. After each measurement, water was restored to the original level by refilling the pipette. In this study, the specimens were tested for 26 days to ensure the steady state flow was achieved. The resulted cumulative water flow was plotted against time.

The water flow through the system is assumed to be continuous and laminar. Therefore, formulation used for calculating the water permeability coefficient k_f (cm/s) can be derived from Darcy's law and are summarized as following:

$$k_f = \left(\frac{a \times l}{A \times t}\right) \ln\left(\frac{h_i}{h_f}\right) \quad \text{(Eq 2)}$$

where k_f is the permeability coefficient (cm/s), A and a are the cross-sectional area of specimen and pipette (cm^2) respectively, L is the specimen thickness (cm), t is the time (s), h_i and h_j are the initial and final water heads, respectively (cm).

2.3.3 Gas Permeability Test. Gas permeability tests were performed using liquid methanol as the gas source to determine the gas transport properties. It was used to shed light on the

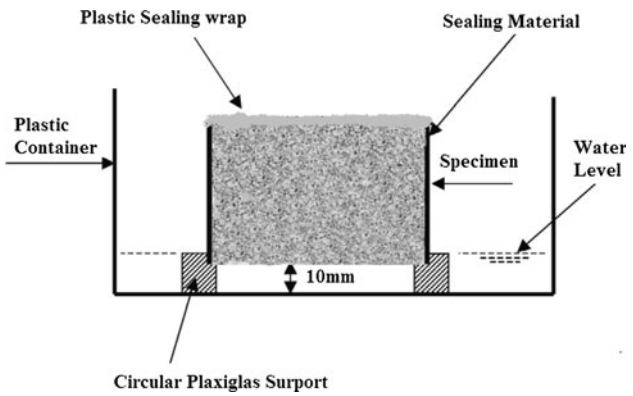

Fig. 1 Experimental setup for water sorptivity test

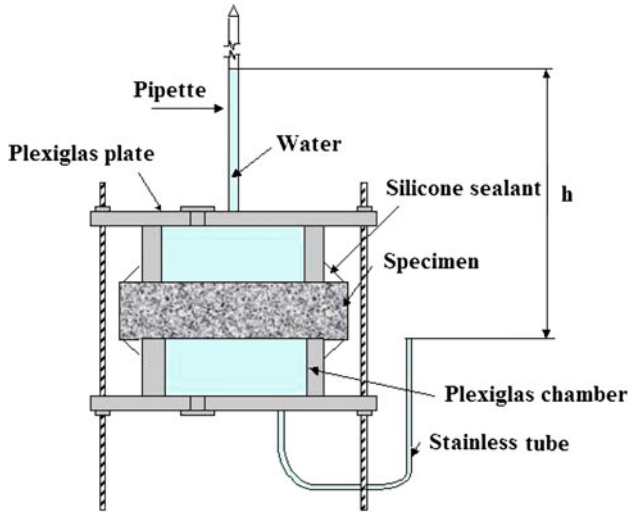

Fig. 2 Experimental setup for water permeability test

effect of CNTs addition on the microstructure of cement-based composites. A 10 mm thick specimen was cut from a 50 × 50 × 50 mm cubic sample and then oven-dried at 105 °C for 24 h to remove the moisture within specimen. Subsequently, the specimen was placed and sealed on the top of a cell with epoxy sealant to avoid any leakage of methanol vapor as shown in Fig. 3. The initial weight of the whole specimen setup including the cell, methanol liquid, specimen, and epoxy sealant was measured at the beginning of the test. The values of mass variation versus time due to the vaporization of methanol liquid at a constant 40 °C water bath temperature during the test were continuously recorded at each time interval until a steady-state mass loss was reached. The gas permeability coefficient k (m^2) was then calculated using the following equations.

$$p_V = 10^{\left(8.0809-\frac{1582.2}{239.76+T}\right)} \quad \text{(Eq 3)}$$

$$\eta = 10^{-7}\left(4.7169T^{0.618} - 99e^{-8.7593\times10^{-4}T} + 94e^{-7.916\times10^{-3}T} + 5\right) \quad \text{(Eq 4)}$$

$$Q = \frac{266\times10^{-3}m'}{10^{\left(8.0809-\frac{1582.2}{239.76+T}\right)}}T \quad \text{(Eq 5)}$$

$$k = \frac{2L\eta P_2 Q}{A\left(P_1^2 - P_2^2\right)} \quad \text{(Eq 6)}$$

where P_V is the absolute pressure of vapor (N/m^2), T is the absolute temperature (K), η is the dynamic viscosity (N/m^2), Q is the volumetric flow rate (m^3/s), m' is the rate of mass loss (g/s), P_1 is the inlet pressure (N/m^2), P_2 is the outlet pressure (N/m^2), L is the length of the sample (m), and A is the cross-sectional area perpendicular to the flow direction (m^2).

3. Results and Discussion

3.1 Water Sorptivity of CNTs-Reinforced Cement-Based Composites

Figure 4 depicts the variations of absorbed water with water absorbing time for three types of cement-based composites. Figure 4(a) shows that the water absorbing amounts of three types of cement-based composites first increase and then stabilize with the increase in water absorbing time. Both CNTs reinforced cement-based composites demonstrate lower amounts of absorbed water than that of plain cement-based composite. Figure 4(b) shows the linear range of the experimental data, which are fitted using Eq 1. The sorptivity coefficients k_s of three types of composites are listed in Table 3. It can be seen from Table 3 that the sorptivity coefficient of plain cement-based composites is twice of that of CNTs-reinforced cement composites. The above results indicate that the use of CNTs decreases the water sorptivity of cement-based materials. The improvement of CNTs to water sorptivity of cement-based composites is mainly due to: (1) the modification of hydration products; (2) refined pore size distribution and reduction of the porosity; and (3) the reduction of autogenous shrinkage (Ref 2, 4, 13, 17, 24). Therefore, the CNTs-reinforced cement-based composites become much more compacted and exhibit lower water sorptivity relative to those non-reinforced plain composites.

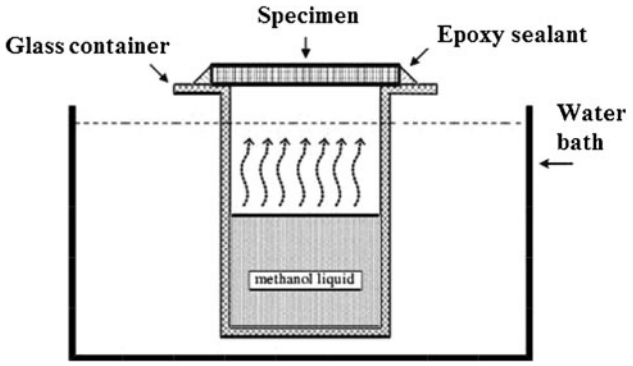

Fig. 3 Experimental setup for gas permeability test

3.2 Water Permeability of CNTs-Reinforced Cement-Based Composites

Figure 5 shows the temporal evolution of cumulative water flow penetrating the cement-based composites. As shown in

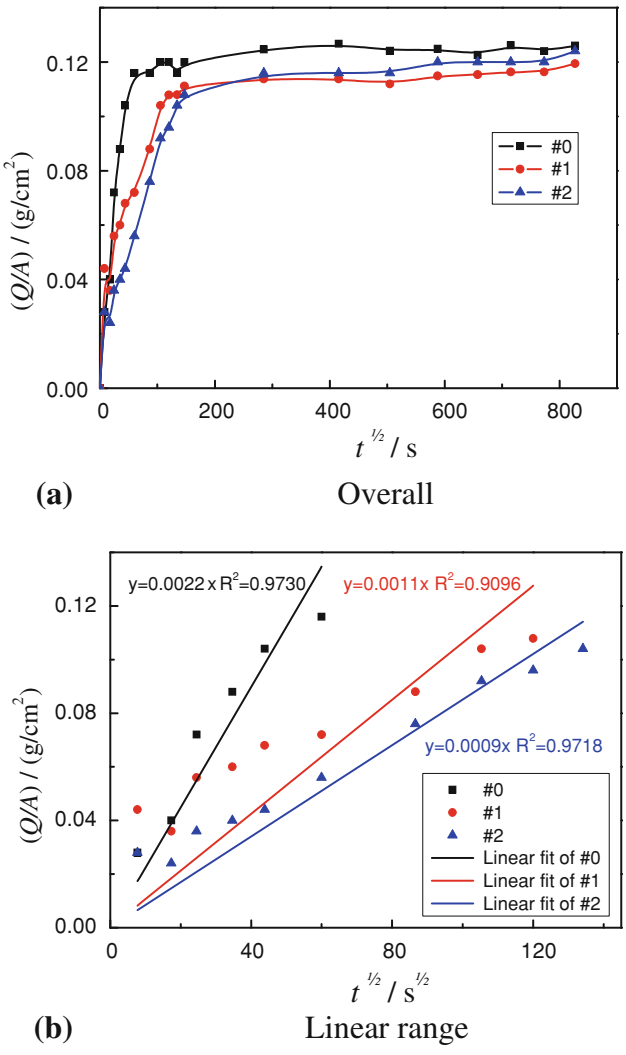

Fig. 4 Relationships between water absorbing amounts and water absorbing time of cement composites with and without MWNTs (#0 = 0% CNT, #1 = 0.2% CNT + NaDDBS, #2 = 0.2% CNT + SDS). (a) Overall and (b) linear range

Fig. 5(a), the cumulative water flow increases with time and the cumulative water flows of both CNTs-reinforced cement-based composites are lower than that of plain cement-based composite. As shown in Fig. 5(a) and (b), the time intervals exhibit a straight line in the permeation cures after 14 days. The permeability coefficients k_f of three types of composites are calculated between 16 and 26 days and are listed in Table 4. It can be seen from Table 4 that the permeability coefficients of CNTs-reinforced cement-based composites are obviously lower than that of the plain cement-based composite. This can also be attributed to the improvement in hydration products, microstructures, and autogenous shrinkage of the cement-based materials by CNTs (Ref 2, 4, 13, 17, 24).

Table 3 Water sorptivity coefficients of three types of cement-based composites

Samples	#0 (0% CNT)	#1 (0.2% CNT + NaDDBS)	#2 (0.2% CNT + SDS)
k_s, g/cm^2·s$^{1/2}$	2.2×10^{-3}	1.1×10^{-3}	9.0×10^{-4}

3.3 Gas Permeability of CNTs-Reinforced Cement-Based Composites

The variations in the loss of methanol with time are illustrated in Fig. 6. As shown in Fig. 6(a), all three types of cement-based composites have the same temporal trends, i.e., the loss of methanol increases with time. Figure 6(b) shows that there is a linear relationship between the loss of methanol and time after 100 min. The rate of mass loss m' and the intrinsic permeability coefficient k of three types of composites can be calculated and

Table 4 Water permeability coefficients of three types of cement-based composites

Samples	#0 (0% CNT)	#1 (0.2% CNT + NaDDBS)	#2 (0.2% CNT + SDS)
k_f, cm/s	9.02×10^{-10}	3.14×10^{-10}	5.16×10^{-10}

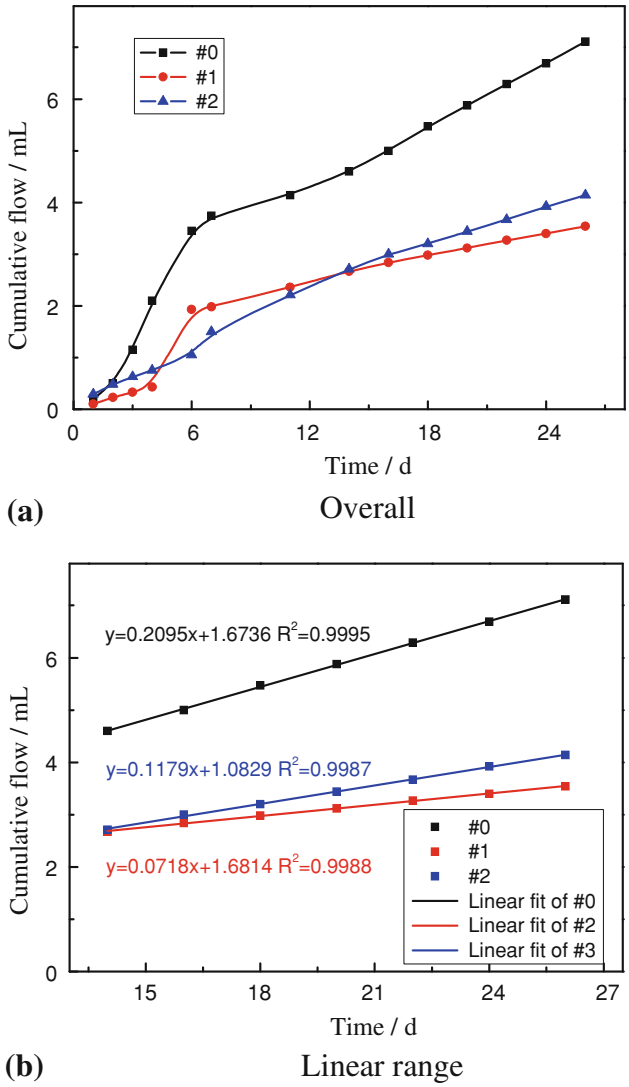

Fig. 5 Relationships between the cumulative water flow and time for cement-based composites with and without MWNTs (#0 = 0% CNT, #1 = 0.2% CNT + NaDDBS, #2 = 0.2% CNT + SDS). (a) Overall and (b) linear range

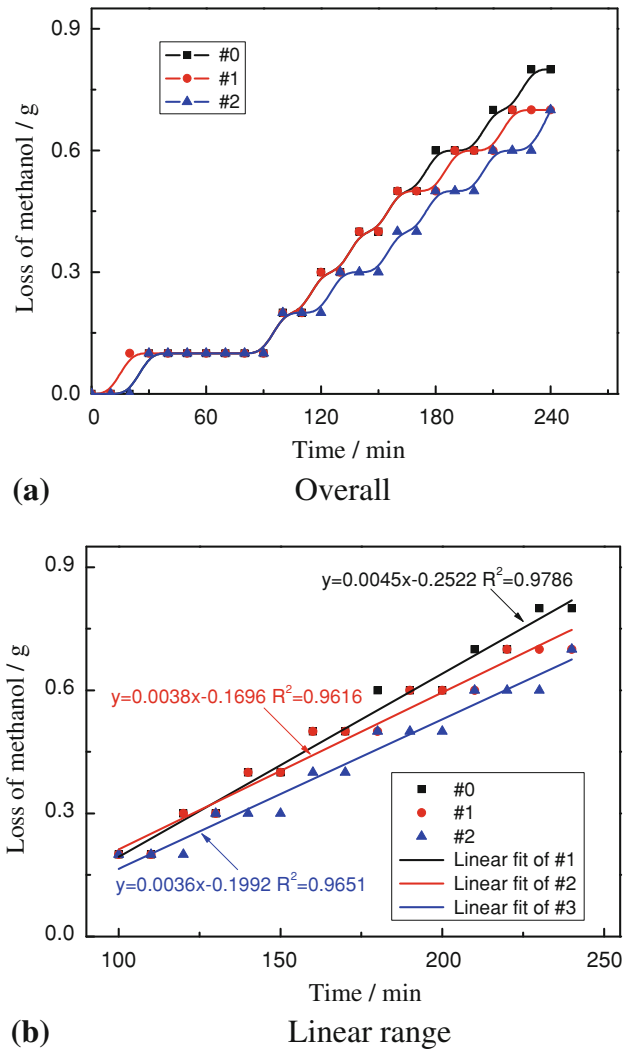

Fig. 6 Relationships between loss of methanol and time for cement-based composites with and without MWNTs (#0 = 0% CNT, #1 = 0.2% CNT + NaDDBS, #2 = 0.2% CNT + SDS). (a) Overall and (b) linear range

Table 5 Gas permeability coefficients of three types of cement-based composites

Samples	#0 (0% CNT)	#1 (0.2% CNT + NaDDBS)	#2 (0.2% CNT + SDS)
m', g/s	0.0045	0.0038	0.0036
k, cm/s	4.00×10^{-17}	3.38×10^{-17}	3.20×10^{-17}

are listed in Table 5. The data indicate that the intrinsic permeability coefficients of CNTs-reinforced cement-based composites are lower than that of the plain cement-based composite. This further proves that the addition of CNTs is beneficial for improving transport properties of the cement-based composites, thus reducing the permeability of the composites.

4. Conclusions

Two kinds of surfactants, SDS and NaDDBS, are used to disperse MWNTs in cement mortar and to facilitate the fabrication of CNTs-reinforced cement mortar composites in this study. The investigations of transport properties (i.e., water sorptivity, water permeability, and gas permeability) of these composites indicate that independent of the surfactant type, the addition of 0.2% MWNTs can decrease water sorptivity coefficient, water permeability coefficient, and gas permeability coefficient, likely through improving the microstructure of the cement-based materials. The findings in this study provide improved understanding of the effect of admixed CNTs on the microstructure and transport properties of cement-based composites. This study adds to the knowledge base relevant to the durability of CNTs-modified cement-based materials.

Acknowledgments

The authors acknowledge the funding support from the Northland Advanced Transportation Systems Research Laboratory (NATSRL) of the University of Minnesota Duluth, ITS of the University of Minnesota, and US National Science Foundation (CMMI-0856477). This work is also partially supported by the National Science Foundation of China (Grant Nos. 50808055, 51178148), the Natural Scientific Research Innovation Foundation in Harbin Institute of Technology (grant No. HIT. NSRIF. 2009096), and the Research and Innovative Technology Administration under the USDOT.

References

1. G. Camps, A. Turatsinze, A. Sellier, G. Escadeillas, and X. Bourbon, Steel-Fibre-Reinforcement and Hydration Coupled Effects on Concrete Tensile Behaviour, *Eng. Fract. Mech.*, 2008, **75**, p 5207–5216
2. S.P. Shah, M.S. Konsta-Gdoutos, and Z.S. Metexa, Highly-Dispersed Carbon Nanotube-Reinforced Cement-Based Materials. US Patent 20090229494A1
3. Z.S. Metaxa, M.S. Konsta-Gdoutos, and S.P. Shah, Crack Free Concrete Made With Nanofiber Reinforcement. Presented at Developing a Research Agenda for Transportation Infrastructure Preservation and Renewal Conference, November 12–13, 2009, Washington, DC, 2009
4. L. Raki, J. Beaudoin, R. Alizadeh, J. Makar, and T. Sato, Cement and Concrete Nanoscience and Nanotechnology, *Materials*, 2010, **3**, p 918–942
5. M.S. Dresselhaus, G. Dresselhaus, and Ph. Avouris, *Carbon Nanotubes: Synthesis, Structure, Properties, and Applications*, Springer, Berlin, Heidelberg, New York, 2000
6. T.W. Odom, J.L. Huang, P. Kim, and C.M. Lieber, Structure and Electronic Properties of Carbon Nanotubes, *J. Phys. Chem. B*, 2000, **104**, p 2794
7. M. Terrones, Science and Technology of the Twenty-First Century: Synthesis, Properties, and Applications of Carbon Nanotubes, *Annu. Rev. Mater. Res.*, 2003, **33**, p 419
8. J. Makar, J. Margeson, and J. Luh, Carbon Nanotube/Cement Composites-Early Results and Potential Applications. *Third International Conference on Construction Materials: Performance, Innovations and Structural Implications*, Vancouver, 2005, p 1–10
9. A. Cwirzen, K. Habermehl-Cwirzen, and V. Penttala, Surface Decoration of Carbon Nanotubes and Mechanical Properties of Cement/Carbon Nanotube Composites, *Adv. Cem. Res.*, 2008, **20**, p 65–73
10. Y.S. De Ibarra, J.J. Gaitero, E. Erkizia, and I. Campillo, Atomic Force Microscopy and Nanoindentation of Cement Pastes with Nanotube Dispersions, *Phys. Status Solidi A*, 2006, **203**, p 1076–1081
11. J.P. Ou and B.G. Han, Piezoresistive Cement-Based Strain Sensors and Self-Sensing Concrete Components, *J. Intell. Mater. Syst. Struct.*, 2009, **20**, p 329–336
12. B.G. Han, X. Yu, and E. Kwon, A Self-Sensing Carbon Nanotube/Cement Composite for Traffic Monitoring, *Nanotechnology*, 2009, **20**, p 445501
13. G.Y. Li, P.M. Wang, and X.H. Zhao, Pressure-Sensitive Properties and Microstructure of Carbon Nanotube Reinforced Cement Composites, *Cement Concr. Compos.*, 2007, **29**, p 377–382
14. J.L. Luo, Fabrication and Functional Properties of Multi-Walled Carbon Nanotube/Cement Composites. Dissertation for the Doctoral Degree in Engineering, Harbin Institute of Technology, Harbin, China, 2009
15. V.P. Veedu, Multifunctional Cementitious Nanocomposite Material and Methods of Making the Same, US Patent 7666327 B1, 2010
16. N.Q. Feng and F. Xing, *Durability of Concrete and Concrete Structure*, China Machine Press, Beijing, 2009
17. S.J. Chen, F.G. Collins, A.J.N. Macleod, Z. Pan, W.H. Duan, and C.M. Wang, Carbon Nanotube-Cement Composites: A Retrospect, *IES J. A*, 2011, **4**(4), p 254–265
18. S. Musso, J.M. Tulliani, G. Ferro, and A. Tagliaferro, Influence of Carbon Nanotubes Structure on the Mechanical Behavior of Cement Composites, *Compos. Sci. Technol.*, 2009, **69**, p 1985–1990
19. L. Vaisman, H.D. Wagner, and G. Marom, The Role of Surfactants in Dispersion of Carbon Nanotubes, *Adv. Colloid Interface Sci.*, 2006, **128–130**, p 37–46
20. J.R. Yu, N. Grossiord, C.E. Koning, and J. Loos, Controlling the Dispersion of Multi-Wall Carbon Nanotubes in Aqueous Surfactant Solution, *Carbon*, 2007, **45**, p 618–623
21. M.F. Islam, E. Rojas, D.M. Bergey, A.T. Johnson, and A.G. Yodh, High Weight Fraction Surfactant Solubilization of Single-Wall Carbon Nanotubes in Water, *Nano Lett.*, 2003, **3**, p 269–273
22. B.B. Sabir, S. Wild, and M. O'Farrell, A Water Sorptivity Test for Mortar and Concrete, *Mater. Struct.*, 1998, **31**(8), p 568–574
23. A.S. El-Dieb, Self-Curing Concrete: Water Retention, Hydration and Moisture Transport, *Constr. Build. Mater.*, 2007, **21**(6), p 1282–1287
24. J.M. Makar and G.W. Chan, Growth of Cement Hydration Products on Single Walled Carbon Nanotubes, *J. Am. Ceram. Soc.*, 2009, **92**, p 1303–1310